Biol. Cybern. 43, 187–198 (1982)

Biological Cybernetics

Theory of Spatial Position and Spatial Frequency Relations in the Receptive Fields of Simple Cells in the Visual Cortex

J.J. Kulikowski[1], S. Marčelja[2], and P.O. Bishop[3]

1 Ophthalmic Optics Department, U.M.I.S.T., Manchester, England

2 Department of Applied Mathematics, Research School of Physical Sciences, Institute of Advanced Studies, Australian National University, Canberra, Australia

3 Department of Physiology, John Curtin School of Medical Research, Institute of Advanced Studies, Australian National University, Canberra, Australia

Abstract. Striate cells showing linear spatial summation obey very general mathematical inequalities relating the size of their receptive fields to the corresponding spatial frequency and orientation tuning characteristics. The experimental data show that, in the preferred direction of stimulus motion, the spatial response profiles of cells in the simple family are well described by the mathematical form of Gabor elementary signals. The product of the uncertainties in signalling spatial position (Δx) and spatial frequency (Δf) has, therefore, a theoretical minimum value of $\Delta x \Delta f = 1/2$. We examine the implications that these conclusions have for the relationship between the spatial response profiles of simple cells and the characteristics of their spatial frequency tuning curves. Examples of the spatial frequency tuning curves and their associated spatial response profiles are discussed and illustrated. The advantages for the operation of the visual system of different relationships between the spatial response profiles and the characteristics of the spatial frequency tuning curves are examined. Two examples are discussed in detail, one system having a constant receptive field size and the other a constant bandwidth.

1. Introduction

Following the discovery that visual neurons have clearly-defined spatial frequency tuning curves (Enroth-Cugell and Robson, 1966; Cooper and Robson, 1968), spatial Fourier analysis has become a well-established method in the study of the responses of cells in the visual system (Movshon et al., 1978a, b; Andrews and Pollen, 1979; Maffei et al., 1979; De Valois et al., 1979; Kulikowski and Bishop, 1981a, b). For the application of Fourier analysis, spatial summation over the cell's receptive field must be linear, or approximately so. The essential linearity of simple cells in the cat striate cortex reported by Movshon et al. (1978a) has been confirmed by Kulikowski and Bishop (1981b).

Preliminary to a linear analysis of the responses of simple cells, Kulikowski et al. (1981) recorded their spatial response profiles to narrow stationary and moving bars and lines that were both brighter and darker than the background and examined the relationship between these responses and those to moving light and dark edges. Then, using the same series of cells, Kulikowski and Bishop (1981b) recorded their responses to stationary and drifting sinusoidal gratings before preparing spatial frequency tuning curves to the drifting gratings. Finally, on the assumption that simple cells operate linearly, the spatial response profiles recorded experimentally were compared with those predicted by inverse Fourier transformation of the spatial frequency tuning curves. Conversely, the spatial frequency tuning curves recorded experimentally were compared with those predicted from the response profiles to moving and stationary stimuli.

The extensive series of experimental observations outlined above suggested the need for a theoretical framework relating the data in the space and spatial frequency domains. The mathematical description of the receptive fields of simple cells in the present paper builds upon the idea that symmetrical and antisymmetrical receptive field types can be considered in terms of the spatial functions obtained by the respective cosine and sine inverse Fourier transforms of the spatial frequency tuning curve (Kulikowski and King-Smith, 1973; Tolhurst, 1977; Movshon et al., 1978a; Kulikowski and Bishop, 1981a, b) and generalizes the description given by Marčelja (1980) in terms of the "elementary signals" of Gabor (1946). A similar set of orthogonal functions (line and edge detectors) was used by King-Smith and Kulikowski to describe

0340-1200/82/0043/0187/$02.40

the detection of one dimensional stimuli including wide bars and space periodic patterns.

In order to give the visual neurophysiologist a better appreciation of the consequences of the mathematical descriptions, spatial sensitivity profiles have been modelled for symmetrical and antisymmetrical receptive fields of cells tuned to different optimal spatial frequencies and bandwidths. In addition a table has been prepared giving the spatial response profiles to bars and edges to be expected from simple cells having a range of different optimal spatial frequencies and bandwidths. Finally, we consider the possible advantages for the visual system of differing relationships between optimal spatial frequency and bandwidth and the corresponding spatial response profiles.

2. Mathematical Description of Receptive Fields

(a) Responses to Narrow Bars and Gratings

The responses of cortical cells depend both on the spatial position of the stimulus as well as the temporal variation in its intensity. Thus, for a light or a dark line, the response will depend not only on the spatial position of the line but also on the magnitude and direction of its velocity. A general linear relationship between the cell response $R(t)$ and the light intensity dependence on spatial position and time $I(x, y, t)$ is given by

$$R(t)=\int dx'dy'dt's(x', y', t-t')I(x', y', t'). \tag{1}$$

The function $s(x, y, t)$ corresponds to the response of the cell at time t to a small spot stimulus briefly flashed at position x, y and time $t=0$. Consider a narrow line stimulus, moving with constant velocity v along the x direction. Then $I(x, y, t)=\delta(x-vt)$ and the response becomes

$$\begin{aligned} R(t)&=\int dx'dy'dt's(x', y', t-t')\delta(x'-vt') \\ &=\int dx'dy's\left(x', y', t-\frac{x'}{v}\right). \end{aligned}$$

The position of the line is given as $x=vt$, and the response expressed as a function of the line position is

$$R(x)=\int dx'dy's\left(x', y', \frac{x-x'}{v}\right). \tag{2a}$$

This expression corresponds to the usual definition of the sensitivity of a cell for a narrow line.

The response of the same cell to sinusoidal gratings of spatial frequency f_0 drifting along the x direction with a constant velocity v_1 is obtained as

$$R(t, f_0)=\int dx'dy'dt's(x', y', t-t')\exp[i2\pi f_0(x'-v_1t')].$$

Complex notation has been used to denote response to cosine and sine gratings. At $t=0$, the response is a function of spatial frequency only, $R(f_0)$. Its Fourier transform is

$$\begin{aligned} R(x)&=2\pi\int dx'dy'dt'df_0s(x', y', -t') \\ &\quad\cdot\exp[i2\pi f_0(x'-v_1t')]\exp[-i2\pi f_0x] \\ &=\int dx'dy's\left(x', y', \frac{x-x'}{v_1}\right). \end{aligned} \tag{2b}$$

In general, this is equal to the response to a moving line (2a) only if the drifting velocity for a grating is equal to the velocity of a moving line.

(b) Responses to Optimally Oriented Stimuli

In the present account we shall limit discussion to the spatial dependence of the cell responses. For a line stimulus moving with a constant velocity, the spatial response profile of a cell obeying linear summation can be described as a function of position, cf. function $R(x)$ of (2a). According to Fourier theory (e.g. Papoulis, 1962) any such function must satisfy the following general relationship between localization in space (within a spatial interval of size Δx) and localization in spatial frequency (within a frequency interval of size Δf).

$$\Delta x\Delta f\geqq 1/2. \tag{3a}$$

The interval size Δx is measured as a root mean square distance from the centre (x_m) of the spatial responsivity profile $s(x)$, i.e.

$$(\Delta x)^2=2\pi\int(x-x_m)^2s^2(x)dx/\int s^2(x)dx$$

and analogously for Δf (Gabor, 1946).

Experimental observations indicate that the receptive fields of simple cortical cells are strongly localized both in spatial position (small receptive field) and in spatial frequency (narrow bandwidth) suggesting a mathematical description whereby the product $\Delta x\Delta f$ in (3a) has its minimal value, i.e.

$$\Delta x\Delta f=1/2. \tag{3b}$$

Such a relationship uniquely requires the receptive fields to have the mathematical form of Gabor elementary signals (Gabor, 1946) with two response profiles $s(x)$ along the x axis across the receptive field, namely:

(a) a *symmetrical* (even symmetrical or cosine) type

$$s_s(x)=\exp\left[-1/2\left(\frac{x-x_0}{\sigma}\right)^2\right]\cos 2\pi f_0(x-x_0); \tag{4a}$$

(b) an *antisymmetrical* (odd symmetrical or sine) type

$$s_a(x)=\exp\left[-1/2\left(\frac{x-x_0}{\sigma}\right)^2\right]\sin 2\pi f_0(x-x_0), \tag{4b}$$

where f_0 is the spatial frequency at which the sensitivity of a cell is maximal, and σ is the standard deviation corresponding to the Gaussian envelope of the sensitivity profile.

Equations (4a) and (4b) are respectively the real and the imaginary parts of a general complex signal obtained as a consequence of the requirement (3b). Any two linearly-independent combinations of the above expressions would also satisfy (3b). Such combinations correspond to a constant phase shift of the cosine and sine factors in (4a) and (4b). After a phase shift, the signals would no longer possess perfect symmetry or antisymmetry. Nevertheless a pair of cells with receptive fields of this kind would record the same amplitude and phase information as a perfectly symmetrical pair. Experimentally Pollen and Ronner (1981) have observed that adjacent simple cells recorded simultaneously with the same electrode in the cat striate cortex were usually tuned to the same stimulus orientation and spatial frequency but had responses that differed in phase by approximately 90°. Two such cells, acting together, would preserve the phase information in the signal.

The above two equations are simplified by assuming that the axis of each receptive field has $x_0=0$ at its centre of symmetry, namely:

$$s_s(x)=\exp\left[-1/2\left(\frac{x}{\sigma}\right)^2\right]\cos 2\pi f_0 x \tag{4c}$$

and

$$s_a(x)=\exp\left[-1/2\left(\frac{x}{\sigma}\right)^2\right]\sin 2\pi f_0 x. \tag{4d}$$

On theoretical grounds receptive fields in the form of Gabor elementary signals, with their maximal responses at different spatial positions (x_0) and at different spatial frequencies (f_0), could transmit all the information obtained in a stimulus with an arbitrary intensity profile. Such a representation is both very *economical* in terms of the number of cells responding to a given stimulus and maximally *efficient* for *stimulus localization.* The latter property is important for ensuring that localized features in the visual scene produce distinct responses without interference from neighbouring regions. The significance of the Gabor representation will be taken up again in Sect. 4.

(c) Receptive Fields in Two Spatial Dimensions

The original Gabor scheme specifies the signal in only one spatial dimension whereas receptive fields are described in two such dimensions. Since simple cortical cells have elongated receptive fields it is natural to use a rectangular coordinate system and to describe the receptive fields in terms of two position variables x and y and two spatial frequency variables f_x and f_y. The Gabor scheme is then easily extended to two dimensions by noting that the mean position and the mean spatial frequency now have both x and y components, i.e.

$$s_s(x,y)=\exp\{-[(x-x_0)^2+(y-y_0)^2]/2\sigma^2\}\cdot\cos[2\pi f_{0x}(x-x_0)+2\pi f_{0y}(y-y_0)]. \tag{5a}$$

The optimal spatial frequency is a vector in the $x-y$ plane. Its magnitude represents the absolute value of the optimal spatial frequency, while its orientation gives the direction across the receptive field. Equation 5a is simplified by choosing the direction of y axis to be along the length of the receptive field, making $f_{0y}=0$

$$S_s(x,y)=\exp\left\{-1/2\left[\left(\frac{x-x_0}{\sigma_x}\right)^2+\left(\frac{y-y_0}{\sigma_y}\right)^2\right]\right\}\cdot\cos[2\pi f_0(x-x_0)]. \tag{5b}$$

The extents to which the receptive field is localized in the x direction across its width and in the y direction along its length are, in general, not equal, and allowance has been made for such an inequality by introducing different standard deviations σ_x and σ_y for the respective profiles. Along the x axis the profiles of the receptive fields consist of the product of a Gaussian envelope and a sine or cosine function. Experimental observations indicate that, along the y axis, the excitatory profile is well fitted by a Gaussian function (Henry et al., 1978). Receptive field profiles of the form of (5b) are shown in Fig. 1.

The description of two-dimensional response profiles by (3) is based on the assumption of linear behaviour by simple cells. This linearity has, however, yet to be systematically tested for non-optimally oriented stimuli. A non-linear suppression may operate for stimuli moving in the y direction along the line of the optimal orientation (Bishop et al., 1973). Nevertheless, for moderate deviations from the optimal orientation, simple cell responses may reasonably be expected to obey the rules of linear summation.

(d) Stimulus Orientation Tuning

The generalization of (1) to two spatial position and two spatial frequency variables provides relationships between the geometrical parameters of the receptive field and the accuracy of the tuning in both spatial frequency and stimulus orientation. The relationships are particularly simple for Gabor receptive fields (5) because of their localization properties expressed in (3b). For two-dimensional elementary signals in rectangular coordinates, (3b) is valid for each direction at right angles, i.e.,

$$\Delta x\Delta f_x=1/2, \tag{3c}$$

$$\Delta y\Delta f_y=1/2. \tag{3d}$$

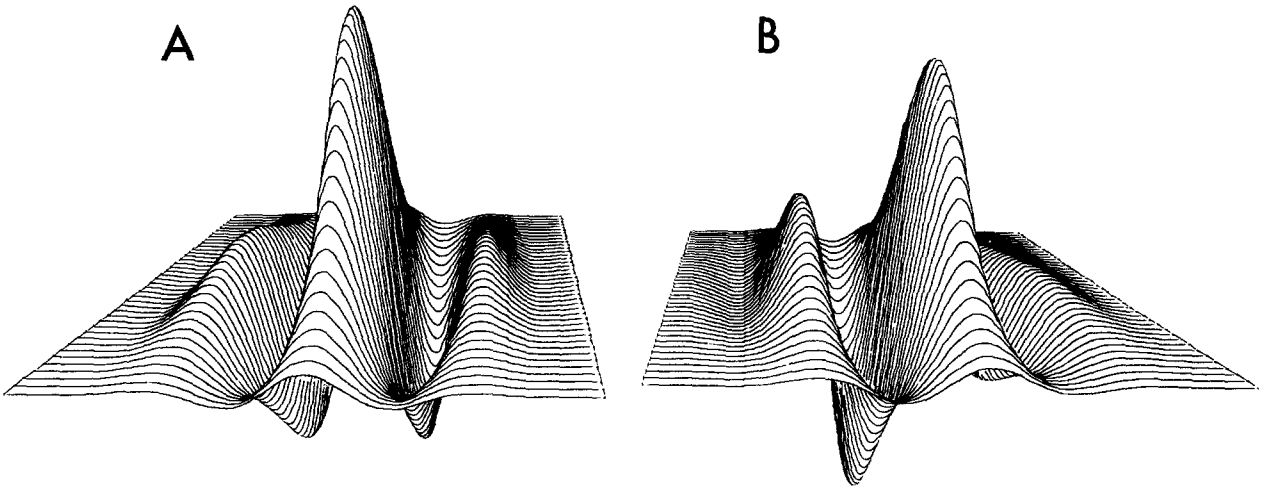

Fig. 1A and B. Examples of the symmetrical and antisymmetrical receptive fields of two simple cells modelled by two-dimensional Gabor elementary signals [e.g. (5b)]. As discussed in Sect. 3, the number of distinct subregions depends on the product $R = f_0 \sigma_x$. In this figure, R was set to 0.51 which is in the range of experimentally-encountered values (cf. Table 1). The ratio $\sigma_x/\sigma_y = 0.55$ corresponds to the orientation tuning curve for the simple cell shown in Fig. 2

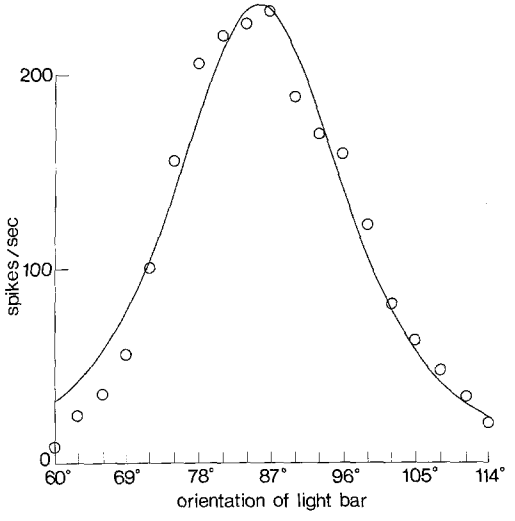

Fig. 2. Continuous line: orientation tuning curve for two-dimensional elementary signals, (7). Open circles: plot of experimentally-recorded responses of a simple cell as a function of stimulus orientation (Henry et al., 1973). The least-squares fit of (7) to the data points determines the ratio $\sigma_x/\sigma_y = 0.55$

The relationship of the uncertainty in spatial position across the receptive field to spatial frequency tuning (3c) is discussed in Sect. 3. The second relationship (3d) provides a connection between the length of the receptive field, the optimal spatial frequency and the sharpness of the stimulus orientation tuning. The vector describing the optimal spatial frequency (f_0) is oriented along the f_x direction. The orientation uncertainty ($\Delta\phi$) associated with the receptive field is geometrically related to the uncertainty in spatial frequency (Δf_y) along the f_y direction as

$$\Delta\phi = \Delta f_y / f_0 . \tag{6}$$

Using (3d) this leads to

$$1/\Delta\phi = 2\Delta y f_0 . \tag{3e}$$

The reciprocal of the orientation uncertainty ($1/\Delta\phi$) is a measure of the sharpness of the orientation tuning and is proportional both to the length of the receptive field and to the optimal spatial frequency associated with that field.

An example of the orientation tuning predicted by two-dimensional receptive fields of the form of (5b) is shown in Fig. 2. For a line stimulus making an angle α with the optimal orientation, the cell response is proportional to the factor

$$\exp[-(2\pi f_0)^2/(1/\sigma_x^2 + \tan^2\alpha/\sigma_y^2)] . \tag{7}$$

This form is compared in Fig. 2 to the orientation tuning data of Henry et al. (1973). Since receptive field characteristics in that case were not independently measured, the ratio $\sigma_x/\sigma_y = 0.55$ was determined from the least-squares fit to the data.

3. Spatial Frequency Tuning Curves and Spatial Sensitivity Profiles

As we have already remarked, the preference shown by simple cells for a particular stimulus orientation makes it possible, in discussions of spatial frequency tuning, to restrict descriptions to one spatial and one spatial frequency dimension (i.e. across the receptive field), thereby considerably simplifying the analytical functions.

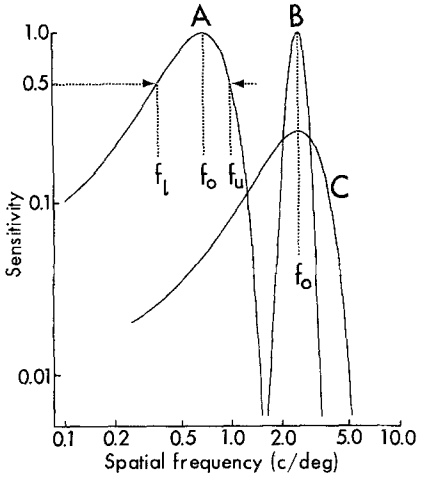

Fig. 3. Spatial frequency tuning curves (*A*, *B*, and *C*) mathematically derived from their respective spatial response profiles in Fig. 4 (*A*, *B*, and *C*) representing the envelopes: *A* $\sigma=0.60$; $f_0=0.67$ c/deg; $B_{df}=0.94$ (medium bandwidth). *B* $\sigma=0.60$; $f_0=2.5$ c/deg; $B_{df}=0.25$ (narrow bandwidth). *C* $\sigma=0.16$; $f_0=2.5$ c/deg; $B_{df}=0.94$ (medium bandwidth). The sensitivites for Curves *A* and *B* are virtually the same. Note that, for $\sigma/X_0 \geqq 0.4$, the sensitivity if virtually determined by σ. For this reason the sensitivity for Curve *C* is 3.75 times reduced

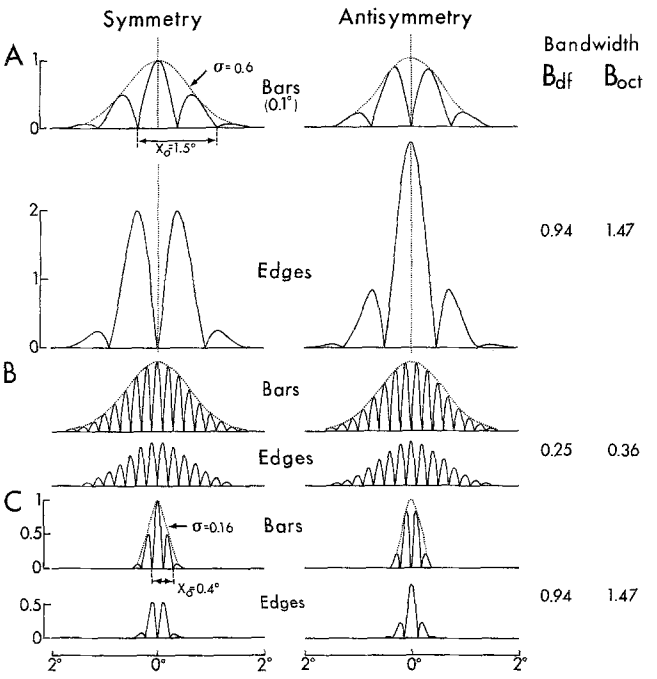

Fig. 4A–C. Theoretically derived spatial sensitivity profiles for bars and edges modelled for symmetrical and antisymmetrical receptive fields of simple cells tuned to optimal spatial frequencies 0.67 c/deg **A** and 2.5 c/deg **B** and **C**. Both positive (ON) and negative (OFF) regions have been shown above the baseline. Note that the optimal spatial frequency (f_0) $=1/X_0$. All the cells are assumed to have equal sensitivity to 0.1° bars. The pairs of profiles represent: **A** Characteristics of an average cell encountered in our experiments that is tuned to *low* spatial frequencies and with a medium bandwidth ($B_{oct}=1.47$; $B_{df}=0.94$; Gabor function with $\sigma/X_0=0.4$). **B** Theoretically postulated characteristics for a model cell tuned to a 3.75 times higher spatial frequency ($f_0=2.5$ c/deg) assuming patch-by-patch analysis but covering the same effective area of the visual field as for **A**. Hence the bandwidth is very narrow ($B_{oct}=0.36$; $B_{df}=0.25$). Note that the symmetrical and antisymmetrical profiles are hardly distinguishable. **C** Theoretically postulated characteristics for a model cell tuned to the same optimal frequency as for **B** but with the same medium bandwidth as in **A**

(a) Spatial Frequency Tuning and Bandwidth

Most simple cells have spatial frequency tuning curves with a single sensitivity maximum (s_0) at the optimal spatial frequency (f_0) and falling off more or less monotonically to either side. A numerical description of the tuning curve is given by the spatial frequency bandwidth (*B*). This bandwidth is commonly defined as the logarithm to the base 2 of the ratio of the upper and lower spatial frequencies (f_u and f_l respectively) at which the sensitivity has fallen to half its maximal value, thus

$$\text{Bandwidth, } B_{oct}=\log_2(f_u/f_l) \tag{8a}$$

with the result expressed in octaves. Thompson and Tolhurst (1979) used another definition of bandwidth that is not expressed in octaves, namely

$$\text{Bandwidth, } B_{df}=(f_u-f_l)/f_0\,. \tag{8b}$$

The above definitions are approximately related as

$$B_{oct}=\log_2\left[1+\frac{f_u-f_l}{f_l}\right]\approx\left[\frac{f_u-f_l}{f_l}\right]\log_2 e\,. \tag{9}$$

Thus B_{oct} approximates 1.44 B_{df} as $(f_u-f_l)\to 0$.

Figures 3 and 4 will be considered in detail below but brief mention of them is needed at this stage. The three spatial frequency (contrast sensitivity) tuning curves (*A–C*) in Fig. 3 have been mathematically derived from their respective spatial sensitivity profiles (A–C) in Fig. 4. The spatial profiles were devised to give two of the tuning curves (*A* and *C*) a medium bandwidth ($B_{df}=0.94$) but with the relatively low (*A*) and fairly high (*C*) optimal spatial frequencies (f_0) of 0.67 and 2.5 c/deg respectively. The remaining curve (*B*) had both a narrow bandwidth ($B_{df}=0.25$) and a high optimal frequency (2.5 c/deg). The numerical values given above and throughout the text are typical of simple cells in the cat striate cortex. The spatial sensitivity profiles for moving bars and edges in Fig. 4 have been modelled for the symmetrical and antisymmetrical receptive field types to show the overall sizes of the receptive fields and the spatial arrangements of the subregions within them as determined by the values of the bandwidths and optimal spatial frequencies of the tuning curves. All the cells are assumed to have equal sensitivity to the 0.1° moving bars.

In Fig. 4 the envelope of the peaks of the individual subregions in each of the spatial sensitivity profiles

given by (4) has a Gaussian form which is described by the first component in the equations, σ being its standard deviation. In order to visualize the significance of σ we can calculate the sensitivities for various values of x in (4). Thus $s=1$ at $x=0$; $s=0.6$ at $x=\sigma$, $s=0.135$ at $x=2\sigma$ etc. If σ is constant, irrespective of the optimal spatial frequency f_0, then the higher the value of f_0 the greater the number of antagonistic subregions that can be confined within the Gaussian envelope, as envisaged in the patch by patch analysis of Robson (1975).

In the theoretical analysis of receptive fields two functions have been found to be especially useful for describing one dimensional spatial frequency tuning curves, namely either the difference between two Gaussian functions or a single Gaussian function.

(b) Difference Between Two Gaussian Functions

The most widely used expression for describing the tuning curve is the difference between two Gaussian functions. A more general expression includes an exponent "n" whose value is made to vary with the bandwidth.

$$S(f)=A[\exp(-af^2)-\exp(-bf^2)]^n, \tag{10}$$

where A is a normalizing coefficient and "a" and "b" are coefficients whose ratio b/a is usually greater than 2.

The difference between two Gaussian functions was originally adopted by Enroth-Cugell and Robson (1966) as a description of the spatial frequency tuning of retinal ganglion cells. For $n=1$ in (10) the tuning curves are rather broad, about 1.8 or more octaves depending upon the ratio b/a. While cells with such a broad bandwidth do occur in the cortex, the majority of cortical cells have tuning curves with bandwidths between 1.3 and 1.5 oct (cf. Movshon et al., 1978b). When the bandwidth is less than 1.5 oct a better description of the tuning curve requires a value of n greater than one and $n=2$ describes tuning curves with a bandwidth between 1.3 oct (for $b/a=2$) and 1.5 oct (for $b/a=3$). For linearly responding cells, such tuning curves predict 5 alternatingly antagonistic subregions for symmetrical receptive fields and 6 subregions for antisymmetrical receptive fields (cf. Fig. 4). The outer subregions would, however, have a rather low sensitivity (below 10% maximum sensitivity), so that their existence or otherwise would probably be revealed only by specially devised tests. Each increase in n in steps of one produces an additional pair of flanking antagonistic subregions. The tuning curves of the narrowest bandwidths described in the literature (0.5 oct or less; DeValois et al., 1978; Movshon et al., 1978b; Thompson and Tolhurst, 1979) would require an n of about 10 and consequently, if the cells were linear, the receptive field would have a great many subregions (cf. Fig. 4). King-Smith and Kulikowski (1975) have evaluated psychophysically the bandwidth of the most sensitive line detecting subunit as not exceeding 1.5 oct.

(c) Single Gaussian Function

A much simpler description of receptive fields with many subregions is provided by a single Gaussian function. A tuning curve having its maximum sensitivity at the optimal spatial frequency f_0 and normalized to $S_0=1$ can be expressed theoretically as:

$$S(f)=\exp[-a(f-f_0)^2], \tag{11}$$

where the coefficient "a" is to be specified after choosing suitable parameters for the description of the spatial sensitivity profiles given by (4a) and (4b) above. Equation (11) has been used to describe a spatial frequency tuning curve for a grating detector (Kulikowski and King-Smith, 1973), but its significance in the theory of communications was earlier stressed by Gabor (1946).

The inverse Fourier transform of (8) predicts two sensitivity profiles along the x axis across the receptive field, namely (4a) and (4b). As shown in Fig. 4 the number of antagonistic subregions that are confined within the Gaussian envelope is determined by the ratio (R) of the standard deviation (σ) to the spatial period (X_0). The spatial period is given by the combined widths of two antagonistic subregions and is the reciprocal of the optimal spatial frequency. Thus:

$$R=\sigma/X_0=\sigma f_0. \tag{12}$$

Fourier transformation of (4a) and (4b) specifies (11) as

$$S_s(f)=\exp\{-2[\pi\sigma(f-f_0)]^2\}\cos[-2\pi x_0(f-f_0)] \tag{13a}$$

and

$$S_a(f)=\exp\{-2[\pi\sigma(f-f_0)]^2\}\sin[-2\pi x_0(f-f_0)] \tag{13b}$$

Note that, in experiments with driftings gratings, if no account is taken of spatial phase only the Gaussian envelope of the Fourier transform (tuning curve) will be available.

By replacing $\sigma=R/f_0$ we obtain

$$S(f)=\exp\{-2[\pi R(f/f_0-1)]^2\}. \tag{14}$$

Simple cells do not respond to diffuse light ($S=0$ at $f=0$), so that the single Gaussian tuning curve can be regarded as valid for these cells whenever R is greater than 0.2. When $R=0.2$ the response at zero spatial frequency (i.e. response to diffuse light) is less than 2% of the response to the optimal spatial frequency,

Table 1. Uncertainties in spatial localization (Δx) and in spatial frequency (Δf)

R	B_{oct}	B_{df}	f_0 (c/deg)	Δx (deg)	Δf (c/deg)	f_0 (c/deg)	Δx (deg)	Δf (c/deg)	f_0 (c/deg)	Δx (deg)	Δf (c/deg)
0.2	4.9	1.87	0.5	0.71	0.71	1	0.35	1.41	2	0.18	2.82
0.3	2.1	1.25	0.5[a]	1.06	0.47	1	0.53	0.94	2	0.26	1.88
0.4	1.47	0.94	0.5[a]	1.41	0.35	1[a]	0.71	0.71	2[a]	0.35	1.41
0.45	1.28	0.83	0.5[a]	1.60	0.31	1[a]	0.80	0.63	2[a]	0.40	1.25
0.5	1.14	0.75	0.5	1.77	0.28	1[a]	0.88	0.57	2[a]	0.44	1.12
0.6	0.94	0.62	0.5	2.12	0.24	1	1.06	0.47	2[a]	0.53	0.94
0.9	0.61	0.42	0.5	3.19	0.16	1	1.60	0.31	2	0.80	0.63
1.2	0.46	0.31	0.5	4.24	0.12	1	2.12	0.24	2	1.06	0.47
1.5	0.36	0.25	0.5	5.31	0.09	1	2.65	0.19	2	1.32	0.37

[a] Denotes cell characteristics approximating those observed experimentally

whereas when $R=0.3$ the response is less than 0.3%. Thus as R increases in steps of 0.1 over a practicable range the response decreases by a factor of about 10 each time.

(d) Bandwidth

At half the maximal sensitivity, (13) and (14) give the upper (f_u) and the lower (f_l) spatial frequency as

$$f_{u,l}/f_0 = 1 \pm \sqrt{\ln 2/2}/\pi R. \quad (15)$$

Depending upon the definition we choose [i.e. (8a) or (8b)], we can derive the bandwidths either in terms of the ratio f_u/f_l or the difference $f_u - f_l$, thus:

$$\begin{aligned} B_{oct} &= \log_2(f_u/f_l) \\ &= \log_2\{[(1+\sqrt{\ln 2/2})/\pi R]/[(1-\sqrt{\ln 2/2})/\pi R]\} \\ &= \log_2[(1+0.1874/R)/(1-0.1874/R)], \end{aligned} \quad (16)$$

$$B_{df} = (f_u - f_l)/f_0 = \sqrt{2\ln 2}/\pi R = 0.3748/R. \quad (17)$$

It can be seen now that R uniquely specifies bandwidth since it is the only variable in either (16) or (17). If, however, R changes from one cell to another, more general equations must be used:

$$B_{oct} = \log_2[(1+0.1874/\sigma f_0)/(1-0.1874/\sigma f_0)] \quad (18)$$

and

$$B_{df} = 0.3748/\sigma f_0. \quad (19)$$

It is worth noting that when the standard deviation (σ) is constant, as assumed by Robson (1975) in his theory of visual information processing by equal patches in a patch by patch analysis, the bandwidth decreases as the optimal spatial frequency increases and could be as narrow as $B_{oct}=0.36$ or $B_{df}=0.25$ (at $R=1.5$) for the highest range of spatial frequencies (Thompson and Tolhurst, 1979).

Table 1 shows the uncertainties in spatial position Δx and spatial frequency Δf to be expected for a range of values of R from 0.2–1.5 and for three values of optimal spatial frequency 0.5, 1.0, and 2.0, respectively. Asterisks alongside certain values of optimal spatial frequency indicate the sets of characteristics approximating those of cells that we have encountered experimentally (Kulikowski and Bishop, 1981b).

(e) Accuracy of Linear Interrelations

A strict test of the linearity of spatial summation is when a "null position" is found at which the presentation of a grating of the optimal spatial frequency does not produce a response (Enroth-Cugell and Robson, 1966). Many simple cells do not pass this test (Movshon et al., 1978; Kulikowski and Bishop, 1981b) but still their responses to gratings and bars show a fairly linear interrelationship akin to those in Figs. 3 and 4. The accuracy with which the Fourier transform of the responses to bars agrees with the experimentally determined spatial frequency tuning curve tells us about the degree of linearity. Kulikowski and Bishop (1981b) found that, for the majority of simple cells, the predicted bandwidth of the tuning curve is within 20% of that determined experimentally if the bars move at velocities close to optimal, whereas the prediction is not as good when it is based on the responses to stationary flashing bars. If stimuli depart from the optimal or conditions intervene that lead to greater nonlinearity, the accuracy of the prediction will be affected, since, in those circumstances, the response profile to bars may reveal fewer subregions in the receptive field (i.e. predict a broader bandwidth) whereas the experimentally-determined tuning curve may change in the reverse direction (i.e. be narrowed). Thus a knowledge of the spatial response profile is needed to be confident of the reliability of the experimentally-determined bandwidth. Unfortunately reports in the literature of cells with a very narrow bandwidth below $B_{oct}=1$ ($B_{df}=0.6$) are not supported by corresponding spatial response profiles which, for such cells, should contain more than 6 subregions.

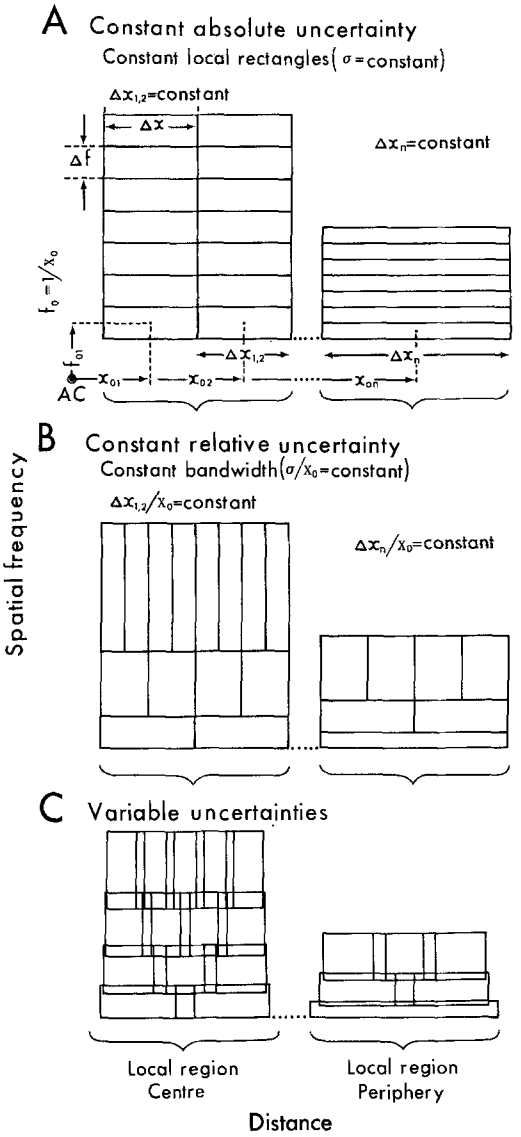

Fig. 5A–C. Three models of possible representations of spatial position and spatial frequency by simple cells in the visual cortex. Models **A** and **B** represent extreme cases in which either absolute or relative uncertainty is kept constant, whereas model **C** is an intermediate case. In all cases the area of the rectangle $\Delta x \Delta f = 1/2$. **A** *System with constant rectangles.* The receptive fields in a given part of the visual field have a constant overall size (constant σ) irrespective of the optimal spatial frequency (f_0). Since both the uncertainties are constant, the rectangles have the same shape at any given eccentricity. **B** *System with constant bandwidth.* The receptive fields in a given part of the visual field have a size that is a constant multiple of the receptive field subregion width (constant σ/X_0). Since, in this case, the uncertainty in spatial localization is directly proportional to subregion width, the rectangles in *B* become correspondingly narrower and longer with an increase in f_0. **C** *Intermediate system with overlap.* Neither absolute nor relative uncertainties are constant since the bandwidth (B_{df}) decreases with increasing f_0, according to a power function in this particular example. In addition the assumption is made that the sampling density is increased so that, with rectangles of a constant area, they must overlap. In this example the overlap has been set at 20%. Note that an overlap is not specially related to system **C**. It could occur in both systems **A** and **B** while still retaining constant absolute and relative uncertainties respectively and both systems remaining extreme cases

4. Relation Between Optimal Spatial Frequency and Bandwidth

The receptive field across its width is characterized by the four parameters: mean position x_0, optimal spatial frequency f_0, uncertainty in spatial position Δx and uncertainty in spatial frequency Δf. Since the experimentally observed spatial frequency tuning curves are Gaussian, (3b) relates the two uncertainties (Δx and Δf) giving the receptive fields least uncertainty in both spatial position and spatial frequency. For each value of x_0 and f_0, there is no mathematical restriction on the value of either one of the two uncertainties but the selection of one uncertainty (e.g. Δf) in the interests of the optimal design of the system would necessarily fix the other (Δx). Furthermore the greater the precision in spatial frequency the poorer the definition in spatial position and vice versa, a circumstance analogous to Heisenberg's (1927) uncertainty principle as pointed out by Gabor (1946) in his analysis of time and frequency in communication theory. It is helpful to show the relationship between the uncertainties in spatial position and spatial frequency in the form of information diagrams (Fig. 5) analogous to Gabor's (1946) representation of elementary signals by logons. In each of the three diagrams A–C in Fig. 5, the individual rectangles, representing the product $\Delta x \Delta f$ in the abstract spatial position-spatial frequency plane ("phase space"), must not be confused with an area (i.e. receptive field) in the visual field.

We may ask what relation between f_0 and Δf would be most advantageous for the operation of the visual system. For a visual recognition task, it would be advantageous if typical stimulus features elicited responses from as few cells as possible. If we were able to decide on a "typical stimulus", it would be possible to determine the most economical sampling scheme in space and in spatial frequency by calculating the Wigner distribution function of the stimulus (Wigner, 1932; Bartelt et al., 1980). This function defines the simultaneous distribution of the associated signal intensities in space and spatial frequency thereby locating those areas in the abstract spatial position-spatial frequency plane of the information diagrams (Fig. 5) where the signals are concentrated. The receptive field parameters x_0, f_0, and Δf can be selected so that the rectangles in Fig. 5 corresponding to the individual receptive fields are shaped to cover only those regions in the spatial position-spatial frequency plane where the Wigner distribution function is substantially different from zero.

To make the analysis less abstract let us consider the three possible systems diagrammed in Fig. 5, namely

(A) System with constant absolute uncertainties (Δx, Δf),

(B) system with constant relative uncertainties $\left(\frac{\Delta x}{X_0}, \frac{\Delta f}{f_0}\right)$,

(C) intermediate system with scatter and redundancy.

Note that the rectangles in Fig. 5 representing the product of the uncertainties have either the same (A) or different (B and C) shapes but their areas (i.e. the product $\Delta x \Delta f$) are in all cases the same.

(a) Constant Absolute Uncertainty

For the two uncertainties, Δx and Δf, to be constant the value of σ must be constant, since $\Delta x = \sigma \sqrt{\pi}$ and $\Delta f = 1/2\sigma \sqrt{\pi}$, and the following relationships hold:

$$\Delta x = \sqrt{(2\ln 2)/\pi}/(f_u - f_l) = \sqrt{(2\ln 2)/\pi}/B_{\mathrm{df}} f_0 . \quad (20)$$

$$\Delta f = \sqrt{\pi/(8\ln 2)}\,(f_u - f_l) = \sqrt{\pi/(8\ln 2)}\,B_{\mathrm{df}} f_0 . \quad (21)$$

When, as in system A, σ is constant, the receptive fields are all of a constant overall size (e.g. Fig. 4A and B) irrespective of the optimal spatial frequency. Thus, for a local region at a given eccentricity, the Δx dimensions in Fig. 5A are all the same. The receptive fields of cortical neurons are, of course, smaller in the centre of gaze and larger in the periphery so that the Δx dimensions in Fig. 5A for the centre are also smaller than those for the periphery.

Another way of looking at system A is that the width of the Gaussian envelope of the spatial sensitivity profile remains the same no matter how many subregions are contained within it (Fig. 4A and B). The large number of subregions in the profiles of Fig. 4B give the impression that, relative to Fig. 4A, the uncertainty in respect to spatial frequency has decreased. However the number of subregions bears a fixed relation to bandwidth and is independent of Δf. Hence, despite the great increase in the number of subregions, Δf remains unchanged, depending only on σ.

Single cells in system A do not maintain great accuracy in spatial localization and cells finely tuned for spatial frequency do not localize in space any better than coarsely tuned cells. For example, in the cat's central visual field at an eccentricity less than 1°, cells with an optimal spatial frequency of 0.5 c/deg would need receptive fields 2° across in order to accommodate two subregions (one cycle $X_0 = 1/f_0$). This would mean that cells tuned to 4 c/deg but with receptive fields of the same size would have 16 subregions corresponding to a bandwidth $B_{\mathrm{df}} = 0.25$ (cf. Appendix). Minimum uncertainty in spatial localization for receptive fields of this size would be about 0.7°. Furthermore with as many as 16 subregions there would be only a few percent difference in sensitivity between the symmetrical and antisymmetrical spatial arrangements (Fig. 5B) requiring considerable precision in the spatial organization of both profiles.

In relation to system A one should also consider how cells with a narrow bandwidth might cover the whole range of spatial frequencies up to the resolution limit which, in the cat, has recently been estimated to be as high as 9 c/deg (Jacobson et al., 1976; Cleland et al., 1979). If only cells with a narrow bandwidth (e.g. $B_{\mathrm{df}} = 0.25$) were to be used, the optimal frequencies for many of them would have to be almost as high as the resolution limit itself. On the other hand less selective cells (e.g. $B_{\mathrm{df}} = 0.6$) tuned to 5 c/deg would cover the same range almost equally well.

(b) Constant Relative Uncertainty

For the two relative uncertainties, $\Delta x/X_0$ and $\Delta f/f_0$, to be constant the bandwidth (B_{df}) must also be constant as follows from equations

$$\Delta x/X_0 = \sqrt{(2\ln 2)/\pi}/B_{\mathrm{df}} \quad (22)$$

and

$$\Delta f/f_0 = \sqrt{\pi/(8\ln 2)}\,B_{\mathrm{df}} . \quad (23)$$

Furthermore if B_{df} is constant $R = \sigma f_0$ must also be constant. This means that the functional form of a given spatial sensitivity profile would be the same regardless of its overall size (e.g. Fig. 4A and C). Thus, for a given constant bandwidth, the sizes of the receptive fields decrease in proportion as the optimal spatial frequencies increase but, depending upon whether the organization is symmetrical or antisymmetrical, the number of subregions remains the same. The receptive fields based on this principle become very small when the subregions become very small. At low spatial frequencies it may not be possible to maintain a system with a relatively narrow bandwidth and having multiple antagonistic subregions since the subregions, and therefore also the receptive fields, would become very large.

System B provides constant relative accuracy both in spatial localization and in spatial frequency selectivity since localization in space is always a fixed multiple of the spatial period. This would be an advantage for an alignment task: the finer the object to be lined up the greater the precision in spatial localization that is required. Nevertheless the system appears to have a disadvantage. While small receptive fields are very good for spatial localization and may have a sensitivity for a line that is equal to that of a large field for the same stimulus they would have a low spatial frequency discriminability for a grating.

Table 2. Responses as a function of bandwidth

$R=\sigma f_0$	Bandwidth		Symmetry				Antisymmetry			
			Bars		Edges		Bars		Edges	
	B_{oct}	B_{df}	No of subregions[a]	% responsivity[a]	No of subregions	% responsivity	No of subregions	% responsivity	No of subregions	% responsivity
0.2	4.9	1.87	3 (3)	100 12.5	2 (2)	100 [0]	2 (2)	100 [1]	1 (1)	100 [0.6]
0.3	2.1	1.25	3 (3)	100 33 [1]	2 (2)	100 [2.4]	4 (4)	100 11 [0.1]	1 (3)	100 (9)
0.4	1.47	0.94	3 (5)	100 50 (6)	4 (4)	100 12 [0.5]	4 (4)	100 25 [1.5]	3 (3)	100 28 [1.5]
0.45	1.28	0.83	5 (5)	100 58 10.9 [0.7]	4 (4)	100 20 [1.1]	4 (4)	100 32 [3.6]	3 (3)	100 39 [4]
0.5	1.14	0.75	5 (5)	100 63 16 [1.6]	4 (4)	100 28 [2.7]	4 (6)	100 40 (6.4)	3 (5)	100 49 (7.9)
0.6	0.94	0.62	5 (7)	100 71 27 (5.3)	4 (6)	100 43 (9)	6 (6)	100 52 14 [1.9]	5 (5)	100 65 19 [2.7]
0.9	0.61	0.42	7 (9)	100 86 55 26 (9)	8 (8)	100 71 37 13 [3.5]	8 (10)	100 67 37 15 [4.5]	7 (9)	100 85 51 23 (7)
1.2	0.46	0.31	11 (11)	100 92 71 46 25 12 [4.6]	10 (12)	100 83 58 34 16 (6.7)	10 (12)	100 84 59 35 18 (8)	11 (11)	100 91 70 45 24 10.5 [4]
1.5	0.36	0.25	13 (15)	100 95 80 61 41 25 14 (6.8)	12 (14)	100 89 71 50 32 18 (9.6)	14 (14)	100 89 72 51 33 19 10 [4.5]	13 (15)	100 94 80 61 40 24 13 (6.5)

[a] No of subregions and % responsivity
without parentheses or brackets $>10\%$
( ) $>5\%<10\%$
[] $<5\%$

The conclusion that this would be a disadvantage is, however, true only for periodic stimuli. Both a narrow line and a sharp edge contain high spatial frequency components that are, however, spread over a broad spatial frequency band. The spatial positions of these stimuli are well defined but they are not tuned to any particular spatial frequency. An analysis using the Wigner distribution function suggests that the information contained in line and edge stimuli is most economically transmitted by a system of cells for which Δf increases with f_0. Thus system A would have the advantage over system B only with respect to those

periodic stimuli in the visual scene that approximate a grating whereas B would have the advantage for the fine non-periodic detail that largely constitutes the natural scene.

(c) Intermediate System with Scatter and Redundancy

Both the data of Thompson and Tolhurst (1979) and that of Kulikowski and Bishop (1981a, b) show no evidence that a single clear-cut, system is in operation. When bandwidth is shown against the optimal spatial frequency on a log-log plot, the regression lines through the two sets of data have the slopes of -0.76 and -0.3, respectively. Although quantitative difference in the slopes of the regression lines is disturbing, qualitatively both sets point to an intermediate system. The considerable scatter in the data points about the regression line of Kulikowski and Bishop (1981a, b) could have arisen from the pooling of data from different systems each of them working over a limited range of spatial frequencies and perhaps operating differently at different eccentricities.

The two systems A and B in Fig. 5 conform to the sampling density required by the sampling theorem. While this retains mathematical elegance, alternative schemes with a degree of redundancy may be more practical. When sampling density is increased beyond the necessary minimum, the rectangles in Fig. 5 with a constant area $\Delta x \Delta f = 1/2$ will begin to overlap (Fig. 5C). The properties of a representation with redundancy in terms of Gabor elementary signals have been studied in quantum chemistry by Davis and Heller (1979). While these authors consider only a system with constant absolute uncertainty, the conclusions they draw are very general and should be valid for any system. Introduction of redundancy (i.e. higher sampling density) improves the convergence of the scheme so that, in the visual system, fewer responding cells would be needed to achieve a given accuracy in the description of a localized stimulus. Introduction of redundancy would also make the representation less sensitive to errors and imperfections in the system.

Appendix

Many investigators record the responses of cortical neurons to moving bars and edges, but not to gratings, so that they have no direct knowledge of the bandwidth of the spatial frequency tuning curves of the cells concerned. Similarly the spatial frequency tuning curves may be recorded but not the responses to bars and edges. Table 2 provides a direct comparison between the two sets of results, the relative values of the amplitudes of the responses of simple cells to bars and edges for various values of $R = \sigma f_0$, and consequently for various values of bandwidth, having been computed using the equations of the symmetrical and antisymmetrical Gabor functions. In each case the amplitude of the response from the subregion giving the strongest response has been normalized to 100. The values without parentheses or brackets are from subregions giving responses with amplitudes greater than 10% of the maximal response. The values enclosed in parentheses are between 5% and 10% of the maximal response, and those in brackets are less than 5%. The values would differ slightly if other equations are used to describe the spatial frequency tuning curves but it is our experience that the results would not be greatly different.

Acknowledgements. We wish to thank Dr. W. R. Levick and Dr. D. A. Pollen for helpful advice and discussion. Our thanks are also due to Mr. K. Collins and Mr. A. L. Johansen for assistance in the preparation of the figures and Miss J. Livingstone and Mrs. E. McNaughton for secretarial assistance.

References

Andrews, B.W., Pollen, D.A.: Relationship between spatial frequency selectivity and receptive field profile of simple cells. J. Physiol. (London) **287**, 163–176 (1979)

Bartelt, H.O., Bremner, K.-H., Lohmann, A.W.: The Wigner distribution function and its optical production. Optics Commun. **32**, 32–38 (1980)

Bishop, P.O., Coombs, J.S., Henry, G.H.: Receptive fields of simple cells in the cat striate cortex. J. Physiol. (London) **231**, 31–60 (1973)

Cleland, B.G., Harding, T.H., Tulunay-Keesey, U.: Visual resolution and receptive field size: examination of two kinds of cat retinal ganglion cell. Science **205**, 1015–1017 (1979)

Cooper, G.F., Robson, J.G.: Successive transformation of spatial information in the visual system. IEE/NPL Conference on pattern recognition, IEE Conference publ. **42**, 134–143 (1968)

Davis, M.J., Heller, E.J.: Semiclassical Gaussian basis set method for molecular vibrational wave functions. J. Chem. Phys. **71**, 3383–3395 (1979)

De Valois, K.K., De Valois, R.L., Yund, E.W.: Responses of striate cortex cells to grating and checkerboard patterns. J. Physiol. (London) **291**, 483–505 (1979)

Enroth-Cugell, C., Robson, J.G.: The contrast sensitivity of retinal ganglion cells of the cat. J. Physiol. (London) **187**, 517–552 (1966)

Gabor, D.: Theory of communication. J. IEE. (London) **93**, 429–457 (1946)

Heisenberg, W.: Über den anschaulichen Inhalt der quantentheoretischen Kinematik und Mechanik. Z. Phys. **43**, 172–198 (1927)

Henry, G.H., Bishop, P.O., Tupper, R.M., Dreher, B.: Orientation specificity and response variability of cells in the striate cortex. Vision Res. **13**, 1771–1779 (1973)

Henry, G.H., Goodwin, A.W., Bishop, P.O.: Spatial summation of responses in receptive fields of single cells in cat striate cortex. Exp. Brain Res. **32**, 245–266 (1978)

Jacobson, S.G., Franklin, K.B.J., McDonald, W.I.: Visual acuity of the cat. Vision Res. **16**, 1141–1143 (1976)

King-Smith, P.E., Kulikowski, J.J.: Lateral interaction in the detection of composite spatial patterns. J. Physiol. (London) **234**, 5–6P (1973)

King-Smith, P.E., Kulikowski, J.J.: The detection of gratings by independent activation of line detectors. J. Physiol. (London) **247**, 237–271 (1975)

Kulikowski, J.J., Bishop, P.O.: Fourier analysis and spatial representation in the visual cortex. Experientia **37**, 160–163 (1981a)

Kulikowski, J.J., Bishop, P.O.: Linear analysis of the responses of simple cells in the cat visual cortex. Exp. Brain Res. (1981b) (in press)

Kulikowski, J.J., King-Smith, P.E.: Spatial arrangement of the line, edge and grating detectors revealed by subthreshold summation. Vision Res. **13**, 1455–1478 (1973)

Kulikowski, J.J., Bishop, P.O., Kato, H.: Spatial arrangements of responses by cells in the cat visual cortex to light and dark bars and edges. Exp. Brain Res. (1981) (in press)

Maffei, L., Morrone, C., Pirchio, M., Sandini, G.: Responses of visual cortical cells to periodic and non-periodic stimuli. J. Physiol. (London) **296**, 27–47 (1979)

Marčelja, S.: Mathematical description of the responses of simple cortical cells. J. Opt. Soc. Am. **70**, 1297–1300 (1980)

Movshon, J.A., Thompson, I.D., Tolhurst, D.J.: Spatial summation in the receptive fields of simple cells in the cat's striate cortex. J. Physiol. (London) **283**, 53–77 (1978a)

Movshon, J.A., Thompson, I.D., Tolhurst, D.J.: Spatial and temporal contrast sensitivity of neurones in areas 17 and 18 of the cat's visual cortex. J. Physiol. (London) **283**, 101–120 (1978b)

Papoulis, A.: The Fourier integral and its applications. New York: McGraw-Hill 1962

Pollen, D.A., Ronner, S.F.: Phase relationships between adjacent simple cells in the visual cortex. Science **212**, 1409–1411 (1981)

Robson, J.G.: Receptive fields: neural representation of spatial and intensive attributes of the visual image. In: Handbook of perception, Vol. 5, pp. 81–112. Carterette, E.C., Friedman, M.P., eds. New York: Academic Press 1975

Thompson, I.D., Tolhurst, D.J.: Variations in the spatial frequency selectivity of neurones in the cat visual cortex. J. Physiol. (London) **295**, 33p (1979)

Tolhurst, D.J.: Symmetry and receptive fields. In: Spatial contrast, pp. 36–38. Spekreijse, H., Van der Tweel, L.H., eds. Amsterdam: North-Holland 1977

Wigner, E.: On the quantum correction for thermodynamic equilibrium. Phys. Rev. **40**, 749–759 (1932)

Received: September 30, 1981

Prof. P. O. Bishop
Department of Physiology
John Curtin School of Medical Research
Australian National University
P. O. Box 334
Canberra City, A.C.T. 2601
Australia